Ab initio studies of high-pressure structural transformations in silica

B. B. Karki and M. C. Warren
Department of Physics and Astronomy, The University of Edinburgh, Edinburgh, EH9 3JZ, United Kingdom

L. Stixrude
Department of Physics and Astronomy, The University of Edinburgh, Edinburgh, EH9 3JZ, United Kingdom and School of Earth and Atmospheric Sciences, Georgia Institute of Technology, Atlanta, Georgia 30332-0340

G. J. Ackland and J. Crain
Department of Physics and Astronomy, The University of Edinburgh, Edinburgh, EH9 3JZ, United Kingdom
(Received 3 September 1996)

Three successive pressure-induced structural transformations of stishovite (rutile-structure SiO_2) to denser phases are predicted by the first-principles pseudopotential method within the local-density approximation. The transition from the rutile to the orthorhombic $CaCl_2$ phase occurs at 47 GPa, the transition from the $CaCl_2$ to the Pnc_2 structure at 98 GPa, and finally the Pnc_2 phase transforms to the pyrite phase at 226 GPa. It is clearly illustrated that the first transition is associated with an elastic instability which arises from the strong coupling between elastic constants and the softening rutile B_{1g} mode. The fully optimized structures of the four polymorphs of silica are obtained as a function of pressure. In addition, all zone-center transverse optic modes of the rutile and $CaCl_2$ phases are determined as a function of pressure. The results are in excellent agreement with available experimental data. [S0163-1829(97)02506-X]

I. INTRODUCTION

Since the discovery of stishovite, a rutile-type polymorph of SiO_2 above 10 GPa, by Stishov and Popova,[1] a number of theoretical and experimental attempts have been made to find further high-pressure modifications of silica. The existence of post-stishovite high-pressure phases of silica would be of substantial geophysical importance as free silica can coexist with (Mg,Fe)O in the lowermost mantle.[2] In addition to its great geological significance, SiO_2 has been extensively used in the electronic devices and glass industries. Recent experiments and theoretical calculations have provided some evidence for high-pressure structural transformations in silica. *In situ* Raman spectroscopy[3] has revealed the rutile-to-$CaCl_2$ transition at about 50 GPa which is much lower than previous *in situ* x-ray-diffraction observation of the transition at pressures of 80–100 GPa.[4] Theoretical predictions also disagree: model calculations[5,6] have predicted that the transition should occur at pressures within the range of 80–200 GPa whereas the linearized augmented plane-wave (LAPW) method and the linear-response calculations based on the density-functional perturbation theory (DFPT) have found the transition at 45 and 64 GPa, respectively.[7,8] Very recently, a pair potential model has suggested that a silica phase with Pnc_2 symmetry should be energetically stable with respect to stishovite and its $CaCl_2$-like modification at pressures above 120 GPa.[6] Further, the stability of the pyrite structure of SiO_2 with respect to stishovite has been suggested by two LAPW calculations at pressures above 60 GPa (Ref. 9) and 156 GPa.[7]

In order to understand in detail the pressure-induced structural behavior, including mainly the phase transitions of silica and solve the issue of the existing controversy among the theoretical predictions of the structural transformations in silica, further high-pressure studies are essential. The rutile-to-$CaCl_2$ transition involves the softening of the c_{11}-c_{12} shear modulus and Raman B_{1g} mode with pressure,[7,8] so studies which involve the optimization of all structural parameters (i.e., the lattice constants and free ionic positions) are very important for a detailed understanding. The full structural optimization also gives a detailed picture of internal compression mechanisms which can now be compared to angle-dispersive powder x-ray diffraction.[10] The Raman modes of silica have been experimentally measured up to about 60 GPa,[3] which covers the pressure range in which the rutile-structured SiO_2 and then the $CaCl_2$-structured SiO_2 are stable. A theoretical reproduction of the experimentally determined pressure response of the vibrational modes of silica would demonstrate further the accurate predictive power of the first-principles computer simulations. Here we study these pressure-induced phase transitions in silica, and vibrational properties of two phases, rutile and $CaCl_2$, by using the first-principles computer simulations which allow an efficient full structural optimization.

The organization of the paper is as follows: In Sec. II we describe the methods for structural optimization and zone-center phonon determination. Section III contains the results for structures, phase transitions, and vibrational properties. In Sec. IV we present discussions of the results. Finally, Sec. V deals with conclusions.

II. COMPUTATIONAL DETAILS

A. Structural optimization

The calculations were performed using the pseudopotential method within the local-density approximation (LDA).[11] The method has already been used to predict accurately high-pressure structural, elastic, and vibrational properties of a

large number of materials. The method involves computation of the self-consistent total energies, Hellman-Feynman forces, and stresses by solution of the Kohn-Sham equations; and the subsequent relaxation of the electrons, ions, and unit cell. The optimized, norm-conserving, nonlocal pseudopotentials generated by the Q_C tuning method[12,13] were used in the Kleinman-Bylander form.[14] The parametrization of Perdew and Zunger was used for the exchange-correlation potential.[15] A plane-wave basis set with a 900 eV cutoff was used to expand the electronic wave functions at the special k points generated by a $4\times4\times4$ Monkhurst-Pack k mesh.[16] A single primitive cell of stishovite (two formula units) required about 3000 plane waves per band at each of six special k points. The finite plane-wave basis set corrections to total energies and stresses[17–20] were included (the Pulay stress $=-6.0$ GPa at equilibrium volume). The corrected total energy and stress differences converged to better than 0.1 meV and 0.02 GPa per unit formula. A preconditioned conjugate gradient scheme was used to relax electrons, conjugate gradients to relax ions, and steepest descents to optimize cell parameters. The details of the method have been given elsewhere.[11,18–20]

B. Zone-center phonon calculation

The zone-center phonons were determined by diagonalizing the dynamical matrix D given by

$$D^{\kappa\kappa'}_{\alpha\beta}=\frac{1}{\sqrt{m_\kappa m_{\kappa'}}}\frac{F_{\alpha\kappa}}{\delta}.$$

Here $F_{\alpha\kappa}$ is the force experienced by the κ ion in the α direction due to a small displacement δ of the κ' ion from equilibrium in the β direction. The computation of the Hellmann-Feynman forces by simulating the primitive cell with one atom displaced from the equilibrium position provides one row of elements in the dynamical matrix. Using symmetry information of the system, four independent displacements were needed to construct the required dynamical matrix in the case of the tetragonal (rutile) phase of silica while six displacements were needed in the case of the orthorhombic $CaCl_2$ phase. Diagonalization of the calculated 18×18 dynamical matrix yielded the frequencies and eigenvectors of 18 zone-center phonons.[19–21] To minimize anharmonic effects, we made positive and negative displacements (with magnitude of 0.005 in fractional coordinates) about equilibrium positions and averaged the corresponding restoring forces; this process did not affect the optic modes significantly but reduced the three acoustic modes to zero. The calculated frequencies correspond to transverse frequencies since the long-range macroscopic polarization fields are not accessible at strictly zero wave vector.

III. RESULTS

A. Stishovite

Stishovite (tetragonal space group $P4_2/mnm$) has three structural parameters: two lattice constants a and c, and one oxygen positional parameter x (the oxygen position is $[x,x,0]$). The rutile structure of silica was optimized at several pressures up to 140 GPa enforcing its tetragonal symmetry throughout the simulations (Fig. 1). The calculated zero-pressure structural parameters are in excellent agreement with experiment[22] (Table I). The slight underestimation (by less than 1.0%) of the lattice constants at zero and pressures up to 20 GPa is partly attributed to the LDA and partly to zero temperature (static) calculations. The LDA is expected to work better at higher pressures since the charge density becomes more uniform under compression. The relatively large differences between our results and the higher-pressure data of Tsuchida and Yagi[4] might also be due to the nonhydrostatic stress conditions of their experiments. The calculated pressure-volume data were fit to the third-order Birch-Murnaghan equation of state (Fig. 2). Our value of 313 GPa for bulk modulus falls within the experimental range [292 to 344 GPa (Refs. 23–25)] and is very close to the

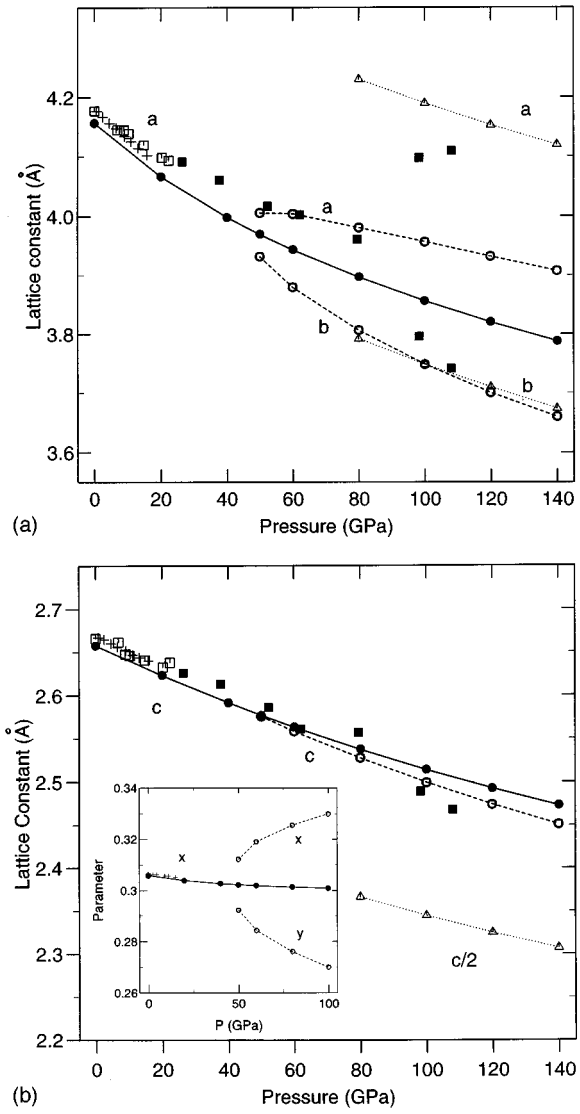

FIG. 1. (a),(b) Lattice constants of three phases of SiO_2; rutile (solid circles), $CaCl_2$ (open circles) and Pnc_2 (triangles). The unit cell of Pnc_2 phase is doubled along the z axis. The experimental data are denoted by open boxes (Ref. 23), solid boxes (Ref. 4), and crosses (Ref. 25), respectively. The inset in (b) shows the oxygen positional parameters: solid circles represent the calculated values for stishovite, open circles those for the $CaCl_2$ phase, and crosses are for the experimental data (Ref. 25).

TABLE I. Zero-pressure structural parameters of stishovite.

	a (Å)	c (Å)	c/a	x	V (Å^3)	K_0 (GPa)	K_0'
This study	4.157	2.658	0.6394	0.3058	45.92	313	4.24
Expt. (Ref. 22)	4.177	2.666	0.6381	0.306	46.60	306±4[a]	3.2±3.3[b]
LAPW (Ref. 7)	4.163	2.664	0.640	0.306	46.16	324	4.04
DFPT (Ref. 8)	4.14	2.66	0.643	0.3052	45.54	320	3.87

[a]Reference 26.
[b]Reference 23.

value (306 GPa) derived from measured single-crystal elastic constants.[26] The experimental value of the pressure derivative K_0' is highly uncertain (Table I).

B. Rutile-to-$CaCl_2$ phase transition in silica

To study the elastic instability in stishovite responsible for the transition to the orthorhombic $CaCl_2$ structure (space group $Pnnm$), the optimized tetragonal unit cell at a given pressure was slightly deformed under an orthorhombic strain and the ionic positions were reoptimized in the strained lattice. Two elastic stiffness constants, c_{11} and c_{12}, of the rutile-structured silica were derived from the computation of stresses generated by the strain. As shown in Fig. 3, the shear modulus c_{11}-c_{12} decreases with pressure, becoming increasingly negative at higher pressures; interpolation gives c_{11}-c_{12}=0 at about 47 GPa, implying that this is the transition pressure. The LAPW and linear-response calculations have shown that c_{11}-c_{12} should vanish at 45 and 64 GPa, respectively.[7,8] The calculated shear modulus c_{11}-c_{12} does not soften with pressure unless the ions are allowed to relax in the deformed cell, indicating a strong coupling between Raman modes and elastic constants (Fig. 3).

An alternative way of investigating the rutile-to-$CaCl_2$ phase transition is to reoptimize the lattice parameters and ion positions of the orthorhombically strained unit cell of the rutile phase at several pressures. Under full structural optimization, at pressures of 0, 20, and 40 GPa, the strained unit cell finally relaxed back to the tetragonal (rutile) phase, whereas at 50 GPa and higher pressures it retained the orthorhombic ($CaCl_2$) phase. We found continuous changes in volume and atomic displacements from the rutile to the $CaCl_2$ structure at the transition (Figs. 1,2), suggesting a second-order phase transition character (i.e., no discontinuity in volume occurs at the transition). The enthalpy of the orthorhombic phase relative to that of the tetragonal phase is zero (on extrapolation) at 47 GPa and then becomes increasingly negative at higher pressures, favoring the $CaCl_2$ structure for silica (Fig. 4). As shown in Fig. 1 the $CaCl_2$ structural parameters: three lattice constants a, b, and c, and two oxygen positional parameters x and y (the oxygen position is $[x,y,0]$) increasingly diverge under compression from the corresponding rutile values suggesting that the degree of the orthorhombic distortion in the $CaCl_2$ structure increases with pressure.

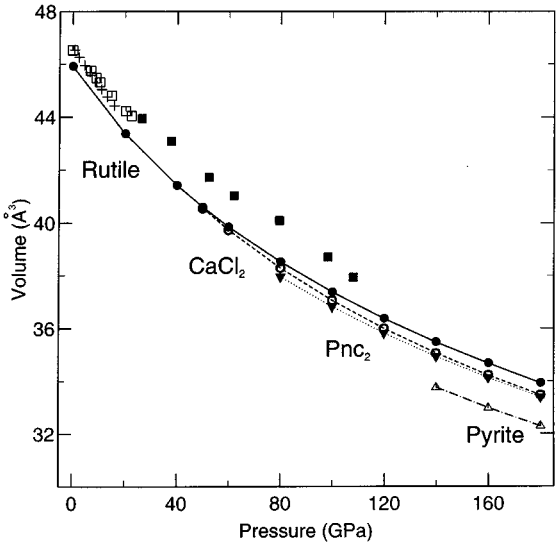

FIG. 2. Volume as function of pressure for four phases of SiO_2; rutile (solid circles), $CaCl_2$ (open circles), Pnc_2 (solid triangles) and pyrite (open triangles). The unit-cell volume is twice that shown here for the Pnc_2 and pyrite phases. The experimental data are denoted as in Fig. 1.

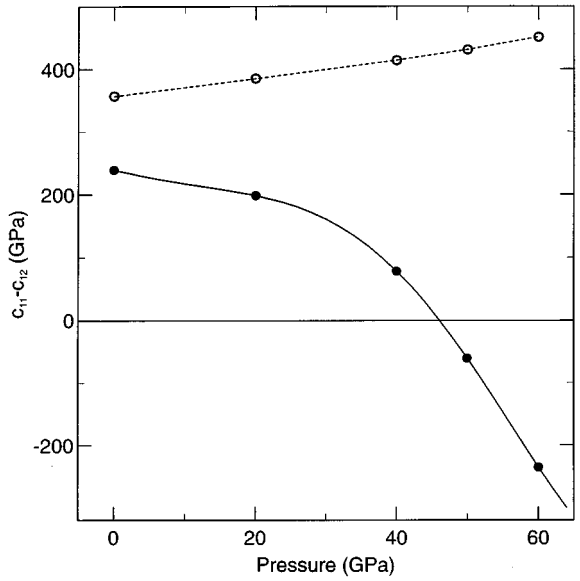

FIG. 3. Pressure dependence of the shear c_{11}-c_{12} of the rutile-structure SiO_2. The solid circles represent the values calculated by allowing the ionic relaxation whereas the open circles those without the ionic relaxation.

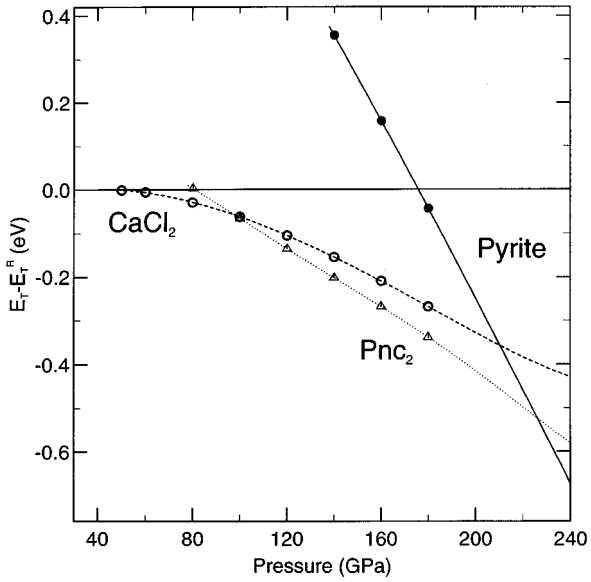

FIG. 4. Free energy (enthalpy $E_T=E+PV$) of the $CaCl_2$ (open circles), Pnc_2 (triangles), and pyrite (solid circles) phases of SiO_2 relative to free energy (E_T^R) of the rutile phase, i.e., (E_T - E_T^R) as function of pressure.

C. $CaCl_2$-to-Pnc_2 phase transition in silica

The possibility of transformation of the $CaCl_2$-type polymorph of silica to a structure with space group Pnc_2 at about 120 GPa has been suggested by pair-potential calculations.[6] From the free-energy (enthalpy) calculations shown in Fig. 4, we found that the $CaCl_2$-to-Pnc_2 phase transition should occur at a lower pressure of 98 GPa. Although there is no experimental observation of this transition, our prediction should be more accurate than the pair-potential method;[6] the latter has also overestimated the rutile-to-$CaCl_2$ transition to be at the relatively high pressure of 83 GPa. The transition involves finite volume collapse and large atomic rearrangements with respect to the $CaCl_2$ phase, indicating a first-order character. The calculated structural parameters over the pressure range from 80 to 140 GPa are shown in Fig. 1 and Table II.

D. Stability of pyrite-structure silica

The transition from stishovite to the pyrite structure (space group $Pa3$) has been addressed by two LAPW calculations which predicted transition at 60 GPa (Ref. 9) and 156 GPa.[7] The reason for the large discrepancy between the two predictions is unknown, though the calculations of Cohen[7] were better converged. We have calculated the structural parameters at 140 GPa to be $a=4.071$ Å and $x=0.348$ for oxygen position $[x,x,x]$. The enthalpy of the pyrite-structure silica was calculated between 140 to 180 GPa, and when compared to that of the other three phases (Fig. 4) suggested a hypothetical transition of the rutile to the pyrite phase at 176 GPa, supporting the LAPW prediction of Cohen.[7] The extrapolation of the calculated enthalpies to higher pressures suggested that the Pnc_2-structure SiO_2 should transform to pyrite-structure SiO_2 at about 226 GPa which exceeds pressures of the Earth's core-mantle boundary.

E. Zone-center phonons of stishovite and $CaCl_2$-structure silica

All zone-center transverse modes (3 acoustic and 15 optic) for the rutile and $CaCl_2$ phases of silica were calculated from 0 to 80 GPa. Three modes with zero frequencies were assigned to the acoustic modes. The calculated eigenvectors were used to deduce the symmetry labels (and hence the irreducible representations) of modes. The rutile optic modes have the irreducible representations:

$$\Gamma_{\text{tetra}}=A_{1g}^{\text{R}}+A_{2g}+A_{2u}^{\text{IR}}+B_{1g}^{R}+B_{2g}^{\text{R}}+2B_{1u}+E_g^{\text{R}}+3E_u^{\text{IR}},$$

whereas the $CaCl_2$ optic modes have the irreducible representations:

$$\Gamma_{\text{ortho}}=2A_g^{\text{R}}+2A_u+2B_{1g}^{\text{R}}+B_{2g}^{\text{R}}+B_{3g}^{\text{R}}+B_{1u}^{\text{IR}}+3B_{2u}^{\text{IR}}+3B_{3u}^{\text{IR}}.$$

The symbols A and B represent nondegenerate, and E doubly degenerate vibrational modes; the symmetric and antisymmetric modes with respect to a center of inversion are denoted by subscripts g and u, respectively; Raman-active modes are indicated by superscript R, infrared active by IR, while the silent modes are unmarked. The optic modes of the two phases were correlated by inspection of the eigenvectors. All Raman-active modes of both phases involve no displacements of silicon ions since they occupy the centrosymmetric positions whereas all infrared-active modes involve silicon sublattice vibration against oxygens.

As shown in Fig. 5, the frequencies of transverse-optic modes of the rutile phase all increase with pressure, except the B_{1g} mode which softens with pressure, whereas all 15 $CaCl_2$ optic frequencies increase with pressure. The softening of the rutile B_{1g} mode with pressure is followed by hardening of the $CaCl_2$ A_g mode with which the rutile B_{1g} mode is correlated, suggesting the rutile-to-$CaCl_2$ phase transition around 47 GPa [Fig. 5(a)]. The frequency of the rutile B_{1g} mode vanishes at a much higher pressure of 86 GPa (on extrapolation). At the transition, the twofold degeneracy of four rutile modes (E_g+3E_u) is lifted and the pressure variations of some modes become discontinuous. The calculated transverse frequencies at zero pressure (Table III)

TABLE II. Internal positional parameters of the Pnc_2 phase of silica.

P (GPa)	Si(1)	Si(2)	O(1)	O(2)
80	(0, 0, 0.1376)	(0.5, 0, 0.8354)	(0.3302, 0.2397, 0.1008)	(0.1698, 0.7397, 0.3723)
100	(0, 0, 0.1370)	(0.5, 0, 0.8358)	(0.3301, 0.2411, 0.1002)	(0.1699, 0.7411, 0.3726)
120	(0, 0, 0.1365)	(0.5, 0, 0.8364)	(0.3299, 0.2423, 0.0998)	(0.1701, 0.7423, 0.3730)
140	(0, 0, 0.1359)	(0.5, 0, 0.8369)	(0.3297, 0.2435, 0.0995)	(0.1703, 0.7435, 0.3733)

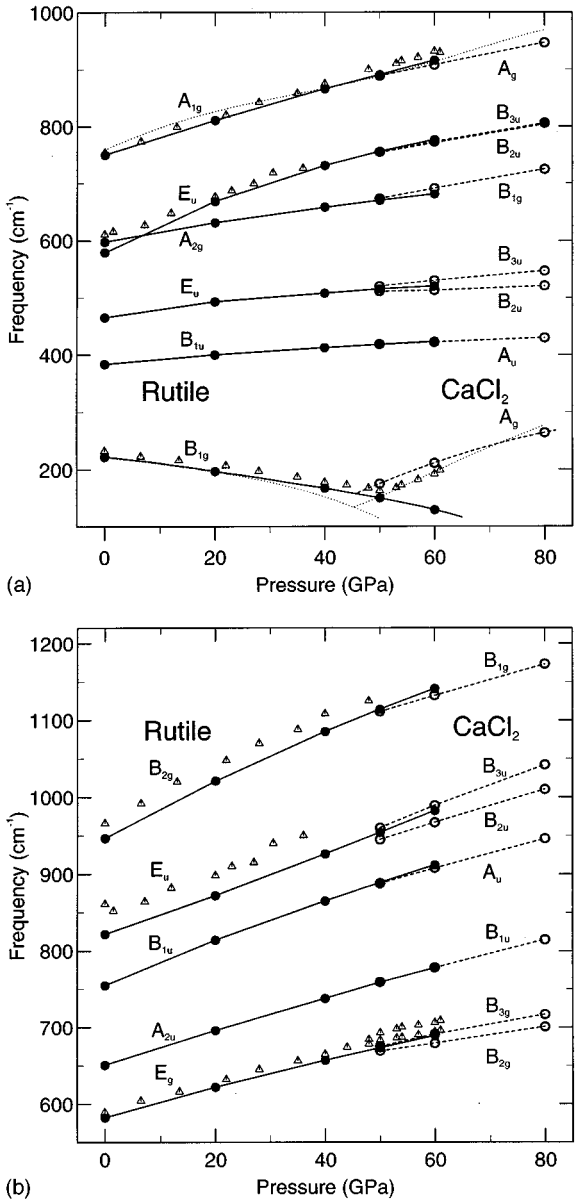

FIG. 5. (a),(b) Zone-center vibrational frequencies of the rutile (solid circles) and $CaCl_2$ (open circles) structures of SiO_2 as function of pressure. The dotted lines are LAPW frozen phonon calculations (Ref. 7). The experimental data for Raman (Ref. 3) and infrared modes (Ref. 29) are denoted by triangles.

and their pressure variations compare favorably with experiments,[3,27–29] and LAPW and linear-response calculations.[7,8,30]

IV. DISCUSSION

Stishovite is comprised of distorted SiO_6 octahedra which share corners in the xy plane and edges in the z direction. The octahedra are distorted in that there are two different Si-O bond lengths (1.752 and 1.796 Å at 0 GPa), three different O-O separations (2.283, 2.510, and 2.658 Å) and one set of the bond angles (98.67°, 81.33°) that depart from the ideal value of 90°. The primary structural response to pressure occurs through the compression of the Si-O and O-O distances (Fig. 6) in agreement with experiments.[25] The SiO_6 octahedra of the rutile structure show a slight decrease in distortion with pressure (corresponding to a slight change in the oxygen position). Similar behavior under compression is shown by the $CaCl_2$ structure, but the degree of the octahedral distortion decreases relatively faster than that in the rutile structure (Fig. 6).

Since the SiO_6 octahedra in both the rutile and $CaCl_2$ structures do not change strongly under compression (in terms of bond lengths and angles), the octahedra may be treated as rigid units.[20,31] The rutile soft-mode eigenvector involves a rotation of the SiO_6 octahedra around the z axis and resembles the displacements of oxygen ions in the orthorhombic phase, relative to their fractional positions in the tetragonal phase (Fig. 7); a corresponding rigid mode was found using the CRUSH package.[31,32] The different lengths of rotation arms in the xy plane of the SiO_6 octahedra require that the tetragonal symmetry is broken for a pure rigid unit mode (Fig. 7). In other words, to maintain rigid unit character under a small rotation angle, one of the lattice parameters must increase slightly, and the other decrease. The rigid unit mode picture provides a natural explanation of the coupling between the B_{1g} mode and the shear modulus c_{11}-c_{12}: when calculating c_{11}-c_{12} without ionic relaxation, the structure cannot access this compression mechanism so the shear modulus remains high (Fig. 3); and without allowing orthorhombic strain, the B_{1g} mode does not soften to zero at the transition [Fig. 5(a)]. Only when both strain and the rota-

TABLE III. Frequencies (cm^{-1}) of zone-center transverse phonons of stishovite (the rutile phase) at 0 GPa and those of the $CaCl_2$-structure silica at 50 GPa compared with experiments [Raman (Ref. 3) and infrared data (Refs. 28 and 29)].

	Rutile phase			$CaCl_2$ phase		
Symmetry	Calc.	DFPT	Expt.	Symmetry	Calc.	Expt.
Raman						
B_{1g}	222	214	232	A_g	174	163[a]
E_g	582	585	589	B_{2g}	669	684
				B_{3g}	675	706
A_{2g}	598	599	Silent	B_{1g}	673	
A_{1g}	750	755	754	A_g	889	906
B_{2g}	947	954	966	B_{1g}	1111	
Infrared						
B_{1u}	383	384	Silent	A_u	418	
E_u	465	469	470	B_{2u}	511	
				B_{3u}	520	
E_u	579	595	580, 611[b]	B_{2u}	754	
				B_{3u}	555	
A_{2u}	651	649	650	B_{1u}	759	
B_{1u}	755	761	Silent	A_u	888	
E_u	822	822	820, 861[b]	B_{2u}	945	
				B_{3u}	960	

[a]Frequency obtained from the broadband is 177 cm^{-1} (Ref. 3).

[b]Frequencies from the transmission and reflection spectra differ significantly depending mainly on particle size and geometry (Ref. 29).

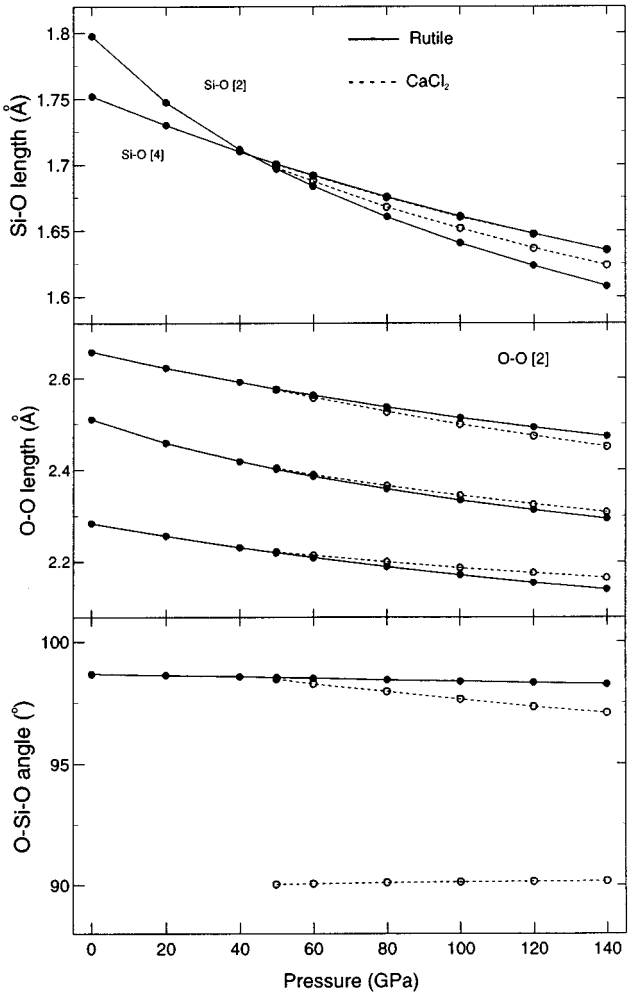

FIG. 6. Si-O and O-O distances, and the O-Si-O bond angles within SiO_6 octahedra in the rutile (solid circles) and the $CaCl_2$ (open circles) phases of silica under pressure.

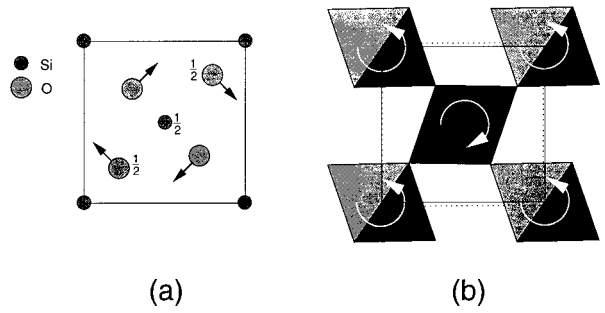

FIG. 7. (a) The eigenvectors of the rutile B_{1g} mode viewed down the z axis; nonzero positions along the z axis are shown. (b) If SiO_6 octahedra rotate as rigid units about the z axis the tetragonal unit cell (dotted line) must distort to an orthorhombic cell (solid line) because the rotation arms in the xy plane of the SiO_6 octahedra have different lengths $[d_1/d_2=2x/(1-2x)=1.57$ at 0 GPa].

tional mode are accessible, is the rigid unit mode possible, which is likely to have low energy and becomes unstable under pressure, driving the transition from the tetragonal (rutile) to the orthorhombic ($CaCl_2$) phase.

The orthorhombic Pnc_2 phase contains four formula units in the unit cell, approximately equivalent to a cell doubling along the z axis relative to the rutile and $CaCl_2$ phases. However, no chains of octahedra parallel to the z axis exist, and more complicated edge-sharing exists, along nonparallel edges. The degree of the octahedral distortion increases with decreasing pressure (from 180 to 80 GPa) and the octahedra tend to transform to seven-apex polyhedra as previously suggested.[6] Similarly, the cubic pyrite phase contains four formula units. Unlike the other phases investigated, there is no edge sharing between octahedra: each oxygen is instead shared between vertices of three octahedra. No rigid unit modes were found using the CRUSH package in either Pnc_2 or pyrite phases.

Our predicted pressure of 47 GPa for the rutile-to-$CaCl_2$ phase transition in silica is in excellent agreement with Raman spectroscopic value[3] of 50 ± 3 and LAPW result[7] of 45 GPa, and is significantly lower than the theoretical predictions based on DFPT (Ref. 8) and model calculations.[5,6] It has now been established quite convincingly that the rutile-to-$CaCl_2$ transition should take place at around 50 GPa. The relatively high transition pressure (80–100 GPa) predicted by the diffraction experiments of Tsuchida and Yagi[4] can be explained in two ways: First, the transition is of second order (at least at 0 K), so the volume changes and atomic displacements from the rutile to the $CaCl_2$ structure at pressures close to the transition point are too subtle to be detected under the nonhydrostatic stress conditions until pressures well beyond the transition; and their experiments are strongly biased by nonhydrostatic stresses. Second, the reinterpretation of the x-ray-diffraction spectra reported by Tsuchida and Yagi did not show any conclusive evidence of the phase transition.[5] Unlike the rutile-to-$CaCl_2$ phase transition, the structural transformation to the Pnc_2 phase and then to the pyrite phase should be clearly observable with x-ray-diffraction experiments since the transition involves appreciable lattice constant changes and atomic displacements. We suggest consideration of both the Pnc_2 and pyrite phases in further high-pressure experimental studies of silica. The possibility of other high-pressure modifications of the Pnc_2 structure before it finally transforms to the pyrite phase at 226 GPa cannot be completely ruled out in the view of the fact that silica undergoes a series of structural transformations [from α-quartz to, coestite, stishovite, $CaCl_2$, and finally to Pnc_2 (Ref. 6)] within the pressure range from 0 to 100 GPa, whereas only one transformation within a more than 100 GPa range has been predicted.

If free silica is present in the Earth's lower mantle (24–136 GPa, 660–2890 km depth), it is expected to exist as stishovite in the uppermost part of this region and to transform to the $CaCl_2$ structure and then to the Pnc_2 structure at greater depths. The transformation from stishovite to the $CaCl_2$ structure will be associated with an elastic anomaly which may be the origin of seismically reflective features in the lower mantle near depths of 1200 km.[3,33] The transition from the $CaCl_2$ structure to the Pnc_2 structure may be asso-

ciated with the seismic reflector at the top of the D'' layer near 2700 km depth.[34]

V. CONCLUSIONS

Starting from stishovite, we predicted three pressure-induced structural transformations in silica up to 240 GPa. The transition from the rutile to the orthorhombic $CaCl_2$ phase occurs at 47 GPa as suggested by the vanishing of the c_{11}-c_{12} shear modulus and the free-energy calculations. The rigid unit mode analysis suggested that the strong coupling between the soft rutile B_{1g} mode and elastic constants is responsible for the rutile-to-$CaCl_2$ phase transition. The transition from the $CaCl_2$ to the Pnc_2 structure occurs at 98 GPa, while the subsequent transition from the Pnc_2 to the pyrite structure occurs at the relatively high pressure of 226 GPa. The predicted stishovite-to-$CaCl_2$ phase transition and the zone-center transverse modes of stishovite and $CaCl_2$ phase at zero and higher pressures are in excellent agreement with experiments.

ACKNOWLEDGMENTS

The authors thank EPSRC for computing facilities under Grant No. GRIK74067, M.C. Payne for the original CASTEP code, M.H. Lee for pseudopotentials, and S.J. Clark for useful discussions. B.B.K. is financially supported by the University of Edinburgh; M.C.W. thanks the EPSRC for support; L.S. acknowledges support from the National Science Foundation under Grant No. EAR-9305060. J.C. acknowledges support from the Royal Society of Edinburgh.

[1] S.M. Stishov and S.V. Popova, Geokhimiya **10**, 837 (1961).
[2] E. Knittle and R. Jeanloz, Science **251**, 1438 (1991).
[3] M.J. Kingma, R.E. Cohen, R.J. Hemley, and H.K. Mao, Nature (London) **374**, 243 (1995).
[4] Y. Tsuchida and T. Yagi, Nature (London) **340**, 217 (1989).
[5] D.J. Lacks and R.G. Gordon, J. Geophys. Res. **98**, 22147 (1993).
[6] A.B. Belonoshko, L.S. Dubrovinsky, and N.A. Dubrovinsky, Am. Miner. **81**, 785 (1996).
[7] R.E. Cohen, *High-pressure Research: Application to Earth and Planetary Sciences* (American Geophysical Union, Washington, DC, 1992), p. 425.
[8] C. Lee and X. Gonze, J. Phys. C **7**, 3693 (1995).
[9] K.T. Park, K. Terakura, and Y. Matsui, Nature (London) **336**, 670 (1988).
[10] M.I. McMahon, R.J. Nelmes, H. Lui, and S. Belmate, High-Press. Res. **14**, 277 (1996).
[11] M.C. Payne, M.P. Teter, D.C. Allan, T.A. Arias, and J.D. Joannopolous, Rev. Mod. Phys. **64**, 1045 (1992).
[12] M.H. Lee, Ph.D. thesis, University of Cambridge, United Kingdom, 1995.
[13] J.S. Lin, A. Qteish, M.C. Payne, and V. Heine, Phys. Rev. B **47**, 4174 (1993).
[14] L. Kleinman and D.M. Bylander, Phys. Rev. Lett. **48**, 1425 (1982).
[15] J.P. Perdew and A. Zunger, Phys. Rev. B **23**, 5048 (1981).
[16] H.J. Monkhurst and J.D. Pack, Phys. Rev. B **13**, 5188 (1976).
[17] G.P. Francis and M.C. Payne, J. Phys. C **2**, 4395 (1990).
[18] B.B. Karki, L. Stixrude, S.J. Clark, M.C. Warren, G.J. Ackland, and J. Crain, Am. Miner. (to be published).
[19] H.C. Hsueh, M.C. Warren, H. Vass, S.J. Clark, G.J. Ackland, and J. Crain, Phys. Rev. B **53**, 14 806 (1996).
[20] M.C. Warren and G.J. Ackland, Phys. Chem. Mineral **23**, 107 (1996).
[21] B.B. Karki, S.J. Clark, M.C. Warren, H.C. Hsueh, G.J. Ackland, and J. Crain, J. Phys. C (to be published).
[22] M.A. Spackman, R.J. Hill, and G.V. Gibbs, Phys. Chem. Mineral **14**, 139 (1987).
[23] L. Lin-gun, W.A. Basset, and T. Takahasi, J. Geophys. Res. **79**, 1160 (1974).
[24] Y. Sato, Earth Planet. Sci. Lett. **34**, 307 (1977).
[25] N.L. Ross, J.F. Shu, R.M. Hazen, and T. Gasparik, Am. Mineral **75**, 739 (1990).
[26] D.J. Weidner, J.D. Bass, A.E. Ringwood, and W. Sinclair, J. Geophys. Res. **87**, B4740 (1982).
[27] R.J. Hemley, H.K. Mao, and E.C.T. Chao, Phys. Chem. Mineral **13**, 285 (1986).
[28] A.M. Hofmeister, J. Xu, and S. Akimoto, Am. Mineral **75**, 951 (1990).
[29] Q. Williams, R.J. Hemley, M.B. Kruger, and R. Jeanloz, Geophys. Res. **98**, 22 157 (1993).
[30] C. Lee and X. Gonze, Phys. Rev. Lett. **72**, 1686 (1994).
[31] A.P. Giddy, M.T. Dove, G.S. Pawley, and V. Heine, Acta. Crystallogr. A **49**, 697 (1993).
[32] K.D. Hammonds, M.T. Dove, A.P. Giddy, and V. Heine, Am. Mineral **79**, 1207 (1994).
[33] L.R. Johnson, Bull. Seism. Soc. Am. **59**, 973 (1969).
[34] M. Weber and J.D. Davis, Geo. J. Inter. **102**, 231 (1990).